Landau damping and resultant unidirectional propagation of chorus waves

J. Bortnik,[1,2] U. S. Inan,[1] and T. F. Bell[1]

Received 2 September 2005; revised 17 November 2005; accepted 28 December 2005; published 3 February 2006.

[1] Using a numerical ray tracing code and a model of the suprathermal electron distribution in the inner magnetosphere, we calculate the Landau damping of chorus waves under realistic conditions. The chorus emissions are assumed to originate at the magnetic equatorial plane with a wave normal angle set at the generalized Gendrin angle, and a wave frequency which is varied from 0.1 to 0.9 of the equatorial electron gyrofrequency. Each ray is propagated until its wave power is diminished by a factor of 10, at which point we record the propagation time, latitude, and the distance along the ray path from the equator. Results indicate that chorus waves are expected to propagate to latitudes of 10°–20° and are typically Landau damped before experiencing magnetospheric reflections, in agreement with satellite observations. In addition, we find longer propagation distances and lifetimes at those frequencies immediately above the half equatorial gyrofrequency and consider the possibility that this effect may contribute to the formation of the two-banded structure of chorus emissions.
Citation: Bortnik, J., U. S. Inan, and T. F. Bell (2006), Landau damping and resultant unidirectional propagation of chorus waves, *Geophys. Res. Lett.*, *33*, L03102, doi:10.1029/2005GL024553.

1. Introduction

[2] Chorus ranks among the most intense natural magnetospheric emissions (typical storm-time average >1 mV/m [*Meredith et al.*, 2001], with peak ~20 mV/m [*Santolik et al.*, 2004]) in the ELF/VLF range (0.3–12.5 kHz), typically occurring as a sequence of continually repeating, short (~0.1 sec) narrowband tones that are usually rising ($df/dt > 0$, occurrence probability P = 77%), falling ($df/dt < 0$, P = 16%), some combination of the above (so-called hooks, regular and inverted, and constant tones, P = 18%) [*Burtis and Helliwell*, 1976], or structureless [*Tsurutani and Smith*, 1974].

[3] Chorus shows several persistent features, most notably occurrence in two distinct frequency bands that peak in power near $0.34f_{ce}$ (lower band) and $0.53f_{ce}$ (upper band), where f_{ce} is the equatorial gyrofrequency along that field-line [*Burtis and Helliwell*, 1976], as well as a wave power minimum near $0.5f_{ce}$ [*Tsurutani and Smith*, 1974], which can reach a width of $0.2f_{ce}$, or occasionally disappear entirely [*Koons and Roeder*, 1990] causing chorus elements to extend from the lower band, through $0.5f_{ce}$, to the upper band. This led *Tsurutani and Smith* [1974] to suggest that an additional process such as Landau damping may be responsible for the observed extinction of chorus wave power in the frequency band near $0.5f_{ce}$.

[4] Nightside chorus is typically confined to a latitudinal range of $|\lambda| < 20°$, with the most intense waves occurring near $\lambda \sim 0°$ [*Tsurutani and Smith*, 1974; *Burtis and Helliwell*, 1976; *Sazhin and Hayakawa*, 1992; *Meredith et al.*, 2001]. Poynting vector analyses of chorus show that propagation is uniformly away from the magnetic equator [*LeDocq et al.*, 1998; *Parrot et al.*, 2003b; *Santolik et al.*, 2004], and recent detailed wave vector analysis [*Lauben et al.*, 2002] shows chorus to be generated preferentially at the Gendrin angle, or high wave normal angles [*Parrot et al.*, 2004] where the source can be moving [*Inan et al.*, 2004].

[5] The propagation of chorus away from the equator suggests that chorus loses wave power before it can magnetospherically reflect (MR) (or specularly reflect from the ionosphere) and propagate back toward the equator. Indeed, a few isolated cases of MR chorus were recently reported by *Parrot et al.* [2003a, 2004], believed to be the first of their kind. Landau damping was proposed as the mechanism responsible for absorbing chorus wave energy [*Burton and Holzer*, 1974; *Goldstein and Tsurutani*, 1984], and in this paper we quantitatively assess whether Landau damping produces the observed features and determine the conditions under which chorus could MR.

2. Method

[6] Using the 2-dimensional Stanford VLF ray tracing code [*Inan and Bell*, 1977] we calculate ray paths representing the chorus emission in the frequency range $0.1f_{rce} < f < 0.9f_{ce}$ and in the L-shell range $4 < L < 8$, with the initial wave normal angle ψ set to the generalized Gendrin angle ψ_G [*Gendrin*, 1961] based on the observations of *Lauben et al.* [2002]. When $\psi = \psi_G$ the wave group velocity vector is parallel to the **B**-field, and the Gendrin angle is approximated by:

$$\psi_G = \begin{cases} \text{undefined} & f < f_{lhr} \\ 90° & f = f_{lhr} \\ \cos^{-1}\left[\dfrac{2\left(f^2 - f_{lhr}^2\right)}{f_{ce} f}\right] & f_{lhr} < f < 0.5f_{ce} \\ 0° & 0.5f_{ce} \le f \le f_{ce} \end{cases} \quad (1)$$

where f_{lhr} is the lower hybrid resonance frequency.

[7] To calculate the path-integrated Landau damping of the ray [*Brinca*, 1972], we use the $f_0(v) = 10f_0^{Bell}$, where f_0^{Bell} is the distribution of 0.1–1.5 keV electrons derived by

[1]Space, Telecommunications, and Radioscience Laboratory, Department of Electrical Engineering, Stanford University, Palo Alto, California, USA.
[2]Department of Atmospheric and Oceanic Sciences, University of California, Los Angeles, California, USA.

0094-8276/06/2005GL024553$05.00

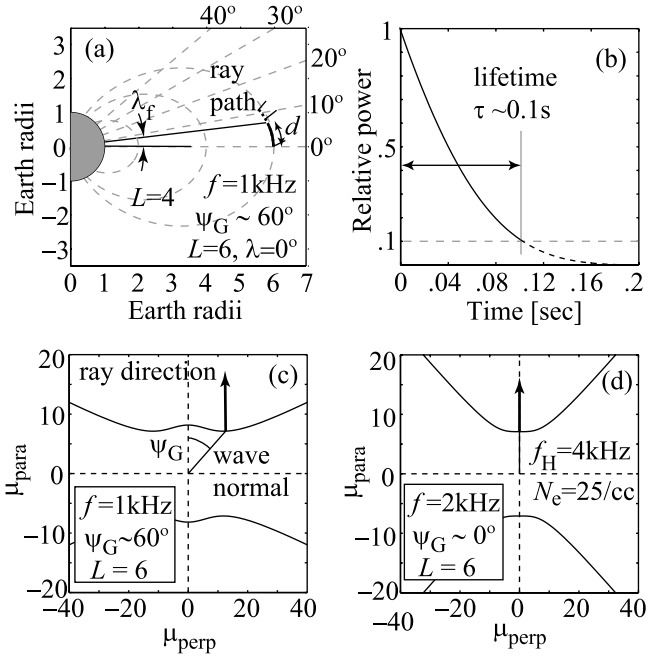

Figure 1. Chorus ray example; (a) ray path of a 1 kHz wave; (b) Landau damping of the ray in (a); (c) initial refractive index surface of the ray in (a); (d) as in (c) but for a 2 kHz ray.

Bell et al. [2002]. Since f_0^{Bell} was measured inside the plasmasphere ($2.3 < L < 4$), it tends to underestimate fluxes outside the plasmasphere. Our scaling ensures that f_0 is comparable to fluxes reported by other authors [e.g., *Korth et al.*, 1999; *Meredith et al.*, 2004] particularly for moderate conditions, near local dawn, and close to the plasmapause, which is the focus of our study. Varying f_0 controls the damping rate and is discussed further in section 4.

[8] Our method is illustrated in Figure 1, where a 1 kHz ($0.25 f_{ce}$) ray is injected at $\lambda = 0°$, $L = 6$, with $\psi = \psi_G \approx 60°$ calculated using (1) ($f_{ce} \approx 4$ kHz). The ray path is shown in a meridional plane in Figure 1a, the relative wave power of the ray as a function of time is shown in Figure 1b, and the refractive index surface of the ray at the injection point is shown in Figure 1c, indicating the Gendrin angle and ray direction. From Figure 1b, we designate the time at which the ray decays to 10% of its initial value as the ray lifetime, τ. The distance over which the ray travels within the time τ is the propagation distance d, and the latitude of the ray at τ is the final latitude λ_f. The quantities τ, d, and λ_f are shown in Figure 1a together with the ray path, the black line segments attached to the ray representing the wave normal at those points. To illustrate how the refractive index surface deforms with frequency, we show in Figure 1d the refractive index surface at the same location as Figure 1c ($L = 6$, $\lambda = 0$), for $f = 2$ kHz $= f_{ce}/2$, but now $\psi_G = 0$.

3. Results

[9] In Figure 2 we show the results of the above analysis, namely d, λ_f, and τ, in Figures 2a, 2b, and 2c, respectively, as a function of f (ordinate) and injection L-shell (abscissa), and note that all rays are injected at $\lambda = 0°$ with $\psi = \psi_G$ calculated using (1). The equatorial electron number density is modeled after *Carpenter and Anderson* [1992], with off-equatorial values distributed in a diffusive equilibrium [*Angerami and Thomas*, 1964]. The plasmapause was located at $L \approx 3.5$ to represent typical conditions, and the geomagnetic field was assumed to be dipolar.

[10] We note from Figures 2a and 2b that d is confined to ~2Re, and $|\lambda_f| < 20°$ except for a narrow band of frequencies above $f_{ce}/2$ which we discuss further below.

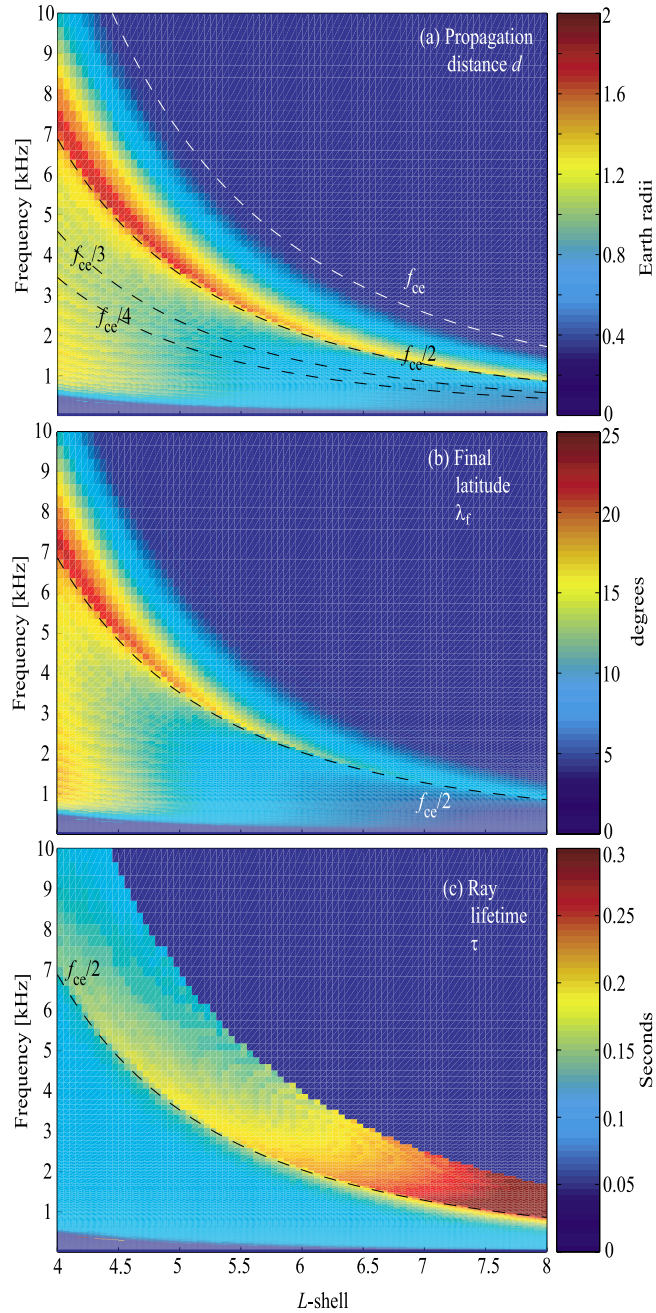

Figure 2. Characteristics of chorus rays injected $\lambda = 0°$, with $\psi = \psi_G$, showing (a) propagation distance d; (b) final latitude λ_f, and (c) ray lifetime τ, for rays injected at L = abscissa value, and f = ordinate value.

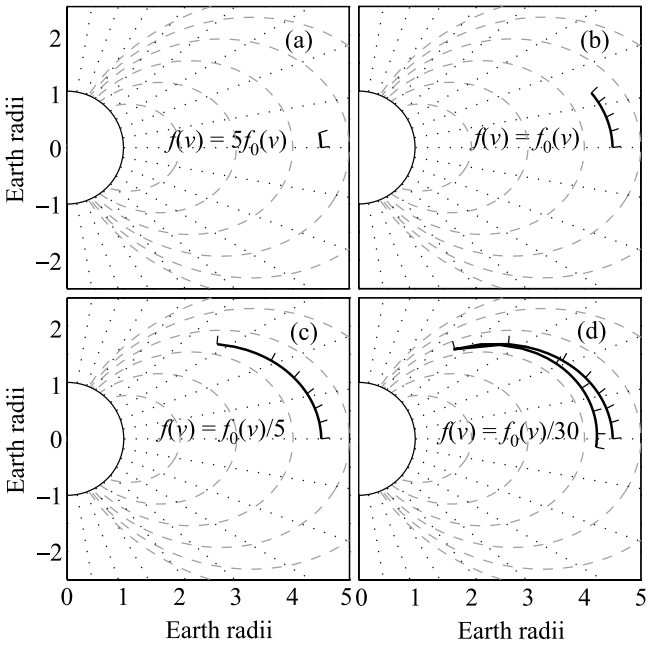

Figure 3. Ray paths of a 700 Hz ray calculated using different $f(v)$, (a) $f(v) = 5f_0(v)$; (b) $f(v) = f_0(v)$; (c) $f(v) = f_0(v)/5$, and (d) $f(v) = f_0(v)/30$ showing MR chorus ray.

This confinement is consistent with observations of night-time chorus near $\lambda \sim 0$ (where typically $|\lambda_f| < 20$ [*Meredith et al.*, 2001; *Tsurutani and Smith*, 1974]). We emphasize that waves only propagate away from the equator and are Landau damped before they MR, accounting for the observed unidirectional propagation [*LeDocq et al.*, 1998; *Parrot et al.*, 2003b; *Santolik et al.*, 2004]. In rare instances, an equatorward propagating chorus element is observed [*Parrot et al.*, 2003a], which we discuss in Section 4.

[11] Figures 2a and 2b show a narrow band of frequencies directly above $f_{ce}/2$ with enhanced values of d and λ_f respectively, at all L-shells. This rather unexpected band comes about due to the topological change in the initial refractive index surface (cf. Figures 1d and 1c) above $f_{ce}/2$ where $\psi_G = 0°$. Since $\psi_G = 0$ at $f = f_{ce}/2$, the wave parallel electric field $E_z^w = 0$ and no Landau damping occurs initially. As the wave propagates away from the equator, gradients in the **B**-field and electron number density increase ψ and hence Landau damping rates. As f increases above $f_{ce}/2$, the rotation to oblique angles accelerates and the ray lifetimes and propagation distance decrease accordingly. We emphasize that this enhancement above $f_{ce}/2$ is not related to wave focusing [*Burtis and Helliwell*, 1976], since we do not consider groups of rays, but only one ray at a time. Instead, the enhancement comes about strictly as a consequence of the behavior of the Landau damping rates as a function of f and the initial ψ_G. We note that the enhancement in d and λ_f is most prominent at lower L-shells, which is consistent with observations of upper-band chorus which occur near the plasmapause [e.g., *Meredith et al.*, 2001; *Lauben et al.*, 2002].

[12] Finally we note that even though d and λ_f decrease monotonically with increasing L-shell, τ tends to increase with L above $f_{ce}/2$ due to the decreasing group velocity. Below $f_{ce}/2$, this decrease in group velocity is balanced by an increase in damping rates, such that lifetimes remain constant at $\tau \sim 0.1$ sec.

4. Discussion

[13] While our simulation clearly shows larger values of τ and d above $f_{ce}/2$ which may be related to the formation of upper-band chorus, a few caveats must be established: firstly, we assume that each ray is injected with $\psi = \psi_G$, an experimental result obtained by *Lauben et al.* [2002]. However, theoretical linear wave growth rates indicate that net growth typically occurs only for $\psi \simeq 0°$ [*Kennel*, 1966; *Brinca*, 1972]. In addition, the suppression in wave power at $f_{ce}/2$ in our simulation only appears at some distance from the equator, whereas the observed suppression occurs much closer to the generation region [*Burtis and Helliwell*, 1976]. These inconsistencies can both be potentially addressed as follows: firstly, if the average temperature of the electrons is increased to several keV, the peak in net growth rate shifts to higher wave normals [*Brinca*, 1972]. Secondly, chorus generation typically occurs slightly off the equator [*Lauben et al.*, 2002; *Santolik et al.*, 2005], and might still occur at $\psi \simeq 0°$, but by the time it propagates to the equator, ψ increases enough to make the chorus wave appear as though it were generated at ψ_G simultaneously suppressing the wave power at $f_{ce}/2$ more effectively. There is also recent evidence that chorus is generated with a spectrum of ψ [*Inan et al.*, 2004] close to the generation region, but ray tracing studies show that only the rays with $\psi \simeq \psi_G$ remain focused for any appreciable distance along the field line [*Lauben et al.*, 2002], whilst wave energy at other angles is strongly defocused in propagating away from the source region. Similarly, only wave normals that lie in the meridional plane are observed [e.g., *Parrot et al.*, 2003a, Figure 2] to remain focused, justifying our use of a 2D ray tracing code. Inclusion of non-linear effects [*Helliwell*, 1995; *Nunn et al.*, 1997; *Trakhtengerts*, 1999] may also account for preferential wave generation at the Gendrin angle, and enhanced suppression of the band at $f_{ce}/2$. In any case, the enhancement of wave power above $f_{ce}/2$ disappears if chorus waves are injected with $\psi = 0$ instead of ψ_G.

[14] Returning to the MR chorus observation [*Parrot et al.*, 2003a, 2004], we note that Landau damping rates depend on the abundance of suprathermal particles, which in turn affect τ, d, and λ_f [*Bortnik et al.*, 2003]. Figure 3 shows a single 700 Hz ray, injected with $\psi = \psi_G$ at $L = 4.5$ (parameters were chosen after the observation of *Parrot et al.* [2004]), and τ calculated using various suprathermal flux distributions, where the ray path is plotted only for the duration of its lifetime τ. We use a multiple of our suprathermal flux distribution f_0 (where $f_0 = 10 f_0^{Bell}$ was used in Figures 1 and 2, and f_0^{Bell} is the suprathermal flux distribution derived by *Bell et al.* [2002]) to represent varying flux levels. Results in Figures 3a–3c show that multiplying f_0 by a factor of 5, 1, and.2, results in $\lambda_f \sim 4°$, $\sim 14°$, and $\sim 32°$ respectively. Continuing along the same lines, in order for the ray to MR and return to the magnetic equator before being extinguished as shown in Figure 3d, the suprathermal particle distribution needs to be $f_0/30$,

which is a reasonable minimum value in the dayside magnetosphere, near the plasmapause. At higher L-shells, $f_0(v)$ needs to be reduced strongly in order to allow a MR to occur. Since suprathermal fluxes actually increase with L-shell [*Meredith et al.*, 2004], the most likely region to observe MR chorus events is thus at low L-shells, directly outside the plasmapause.

[15] In addition, since suprathermal electrons are convected from the magnetotail and drift around the dawn side of the Earth [e.g., *Korth et al.*, 1999] toward local noon, Figure 3 also demonstrates an important local time effect upon wave propagation. The lifetimes of ~1 keV particles are much shorter than their drift period around the Earth [*Chen et al.*, 2005], and thus are strongest near local midnight, and become progressively weaker as they drift to the dayside, resulting in propagation characteristics that qualitatively correspond to Figures 3a, 3b, 3c, and 3d. In agreement with our qualitative assessment, the observation of the MR chorus element by *Parrot et al.* [2003a, 2004] was made on the dayside, at perigee ($L \sim 4.5$). For local times closer to noon, the peak in the distribution of chorus wave power moves to higher latitudes [*Meredith et al.*, 2001] and is thus topologically different to nightside chorus which is the focus of our current paper.

5. Conclusions

[16] Using the Stanford VLF ray tracing code [*Inan and Bell*, 1977], we calculated the ray paths, lifetimes, propagation distances, and final latitudes of rays representing typical chorus elements, injected at $\lambda = 0°$, $4 < L < 8$, $0.1f_{ce} < f < 0.9f_{ce}$, and $\psi = \psi_G$. Our results show that:

[17] 1. Using a typical average suprathermal electron distribution, chorus elements propagate to latitudes of ~10° – 20° and are Landau damped before they are able to MR, resulting in Poynting vectors which only point away from the equator, in agreement with observations [e.g., *LeDocq et al.*, 1998].

[18] 2. When the suprathermal flux distribution is varied, representing the decay of supratheramal fluxes with local time in their drift path around the Earth – the propagation distance is affected such that on the dayside the fluxes may be sufficiently low to permit a magnetospheric reflection of chorus, as reported in a few isolated cases [*Parrot et al.*, 2003a, 2004].

[19] 3. Larger values of τ, d, and λ_f were observed in a frequency band directly above $f_{ce}/2$, which may contribute to the formation of the upper-band in the double banded chorus emission. The validity of this result rests directly on the validity of the assumption that chorus emissions are generated at the Gendrin angle, which has been recently reported [*Lauben et al.*, 2002] and needs to be studied further both experimentally and theoretically.

[20] While our results do not indicate the formation of a distinct lower chorus band, this lower band may be simply formed due to the cutoff at $f_{ce}/2$ on the upper end, and the lack of resonant, anisotropic electron fluxes at higher-energy that are responsible for the wave generation at lower frequencies.

[21] **Acknowledgment.** This research was sponsored by the National Aeronautics and Space Administration (NASA) under grant NAG5-11821-0002, by the Air Force Office of Scientific Research (AFOSR) under grant F49620-03-1-0338, and also by NASA through subcontract via the University of Iowa under grant 4000083338-4 for the POLAR mission and under grant 4000061641 for the CLUSTER mission.

References

Angerami, J. J., and J. O. Thomas (1964), Studies of planetary atmospheres: 1. Distribution of electrons and ions in Earth's exosphere, *J. Geophys. Res.*, *69*(21), 4537–4560.

Bell, T. F., U. S. Inan, J. Bortnik, and J. D. Scudder (2002), The Landau damping of magnetospherically reflected whistlers within the plasmasphere, *Geophys. Res. Lett.*, *29*(15), 1733, doi:10.1029/2002GL014752.

Bortnik, J., U. S. Inan, and T. F. Bell (2003), Energy distribution and lifetime of magnetospherically reflecting whistlers in the plasmasphere, *J. Geophys. Res.*, *108*(A5), 1199, doi:10.1029/2002JA009316.

Brinca, A. L. (1972), On the stability of obliquely propagating whistlers, *J. Geophys. Res.*, *77*(19), 3495–3507.

Burtis, W. J., and R. A. Helliwell (1976), Magnetospheric chorus: Occurrence patterns and normalized frequency, *Planet. Space Sci.*, *24*(11), 1007–1024.

Burton, R. K., and R. E. Holzer (1974), The origin and propagation of chorus in the outer magnetosphere, *J. Geophys. Res.*, *79*(7), 1014–1023.

Carpenter, D. L., and R. R. Anderson (1992), An ISEE/whistler model of equatorial electron-density in the magnetosphere, *J. Geophys. Res.*, *97*(A2), 1097–1108.

Chen, M. W., M. Schulz, P. C. Anderson, G. Lu, G. Germany, and M. Wüest (2005), Storm time distributions of diffuse auroral electron energy and X-ray flux: Comparison of drift-loss simulations with observations, *J. Geophys. Res.*, *110*, A03210, doi:10.1029/2004JA010725.

Gendrin, R. (1961), Le guidage des whistlers par le champ magnetique, *Planet. Space Sci.*, *5*, 274–282.

Goldstein, B. E., and B. T. Tsurutani (1984), Wave normal directions of chorus near the equatorial source region, *J. Geophys. Res.*, *89*(A5), 2789–2810.

Helliwell, R. A. (1995), The role of the Gendrin mode of VLF propagation in the generation of magnetospheric emissions, *Geophys. Res. Lett.*, *22*(16), 2095–2098.

Inan, U. S., and T. F. Bell (1977), The plasmapause as a VLF wave guide, *J. Geophys. Res.*, *82*(19), 2819–2827.

Inan, U. S., M. Platino, and T. F. Bell (2004), Cluster measurements of rapidly moving sources of ELF/VLF chorus, *J. Geophys. Res.*, *109*, A05214, doi:10.1029/2003JA010289.

Kennel, C. (1966), Low-frequency whistler mode, *Phys. Fluids*, *9*(11), 2190–2202.

Koons, H. C., and J. L. Roeder (1990), A survey of equatorial magnetospheric wave activity between 5 and 8 R_E, *Planet. Space Sci.*, *38*(10), 1335–1341.

Korth, H., M. F. Thomsen, J. E. Borovsky, and D. J. McComas (1999), Plasma sheet access to geosynchronous orbit, *J. Geophys. Res.*, *104*(A11), 25,047–25,061.

Lauben, D. S., U. S. Inan, T. F. Bell, and D. A. Gurnett (2002), Source characteristics of ELF/VLF chorus, *J. Geophys. Res.*, *107*(A12), 1429, doi:10.1029/2000JA003019.

LeDocq, M. J., D. A. Gurnett, and G. B. Hospodarsky (1998), Chorus source locations from VLF Poynting flux measurements with the Polar spacecraft, *Geophys. Res. Lett.*, *25*(21), 4063–4066.

Meredith, N. P., R. B. Horne, and R. R. Anderson (2001), Substorm dependence of chorus amplitudes: Implications for the acceleration of electrons to relativistic energies, *J. Geophys. Res.*, *106*(A7), 13,165–13,178.

Meredith, N. P., R. B. Horne, R. M. Thorne, D. Summers, and R. R. Anderson (2004), Substorm dependence of plasmaspheric hiss, *J. Geophys. Res.*, *109*, A06209, doi:10.1029/2004JA010387.

Nunn, D., Y. Omura, H. Matsumoto, I. Nagano, and S. Yagitani (1997), The numerical simulation of VLF chorus and discrete emissions observed on the Geotail satellite using a Vlasov code, *J. Geophys. Res.*, *102*(A12), 27,083–27,098.

Parrot, M., O. Santolik, N. Cornilleau-Wehrlin, M. Maksimovic, and C. Harvey (2003a), Magnetospherically reflected chorus waves revealed by ray tracing with CLUSTER data, *Ann. Geophys.*, *21*, 1111–1120.

Parrot, M., O. Santolik, N. Cornilleau-Wehrlin, M. Maksimovic, and C. C. Harvey (2003b), Source location of chorus emissions observe by CLUSTER, *Ann. Geophys.*, *21*, 473–480.

Parrot, M., O. Santolik, D. A. Gurnett, J. S. Pickett, and N. Cornilleau-Wehrlin (2004), Characteristics of magnetospherically reflected chorus waves observed by CLUSTER, *Ann. Geophys.*, *22*, 2597–2606.

Santolik, O., D. A. Gurnett, and J. S. Pickett (2004), Multipoint investigation of the source region of storm-time chorus, *Ann. Geophys.*, *22*, 2555–2563.

Santolik, O., D. A. Gurnett, J. S. Pickett, M. Parrot, and N. Cornilleau-Ehrlin (2005), Central position of the source region of storm-time chorus, *Planet. Space Sci.*, *53*, 299–305.

Sazhin, S. S., and M. Hayakawa (1992), Magnetospheric chorus emissions: A review, *Planet. Space Sci.*, *40*(5), 681–697.

Trakhtengerts, V. Y. (1999), A generation mechanism for chorus emission, *Ann. Geophys.*, *17*, 95–100.

Tsurutani, B. T., and E. J. Smith (1974), Postmidnight chorus: A substorm phenomenon, *J. Geophys. Res.*, *79*(1), 118–127.

T. F. Bell and U. S. Inan, Space, Telecommunications, and Radioscience Laboratory, Department of Electrical Engineering, Stanford University, 350 Serra Mall, Stanford, CA 94305, USA.

J. Bortnik, Department of Atmospheric and Oceanic Sciences, Math Sciences Building, Room 7115, University of California, Los Angeles, CA 90095, USA. (jbortnik@gmail.com)